

The Angular Scale of Topologically-Induced Flat Spots in the Cosmic Microwave Background Radiation

David Olson and Glenn D. Starkman

Dept. of Physics, Case Western Reserve University, Cleveland, OH 44106

March 24, 2022

Abstract

The notion that the topology of the universe need not be that of the universal covering space of its geometry has recently received renewed attention [5]. Generic signatures of cosmological topology have been sought, both in the distribution of objects in the universe, and especially in the temperature fluctuations of the cosmic microwave background radiation (CMBR). One signature[1], identified in the horn topology but hypothesized to be generic[1, 2] is featureless regions or flat spots in the CMBR sky. We show that typical observation points within the cusped 3-manifold m003 from the Snappea census[3] have flat spots with an angular scale of about five degrees for $\Omega_0=0.3$. We expect that this holds for other small volume cusped manifolds with this Ω_0 value.

1 Introduction

Recently, there has been considerable interest in the prospect that the universe has non-trivial topology. This heightened awareness of the possibility of topology has been driven by the ever strengthening case against a flat, matter dominated universe. The two alternatives which best fit the data are either a flat, cosmological constant dominated universe, or a negatively curved, matter dominated universe. If the universe has negative curvature, then the curvature scale is also the natural scale on which one would generically expect topology.

Since the curvature scale of a negatively curved universe

$$R_c \simeq \frac{3000h^{-1}}{\sqrt{1-\Omega}} \text{Mpc} \quad (1)$$

is considerably less than the radius of the observable universe, one might hope to be able to observe evidence for the non-trivial topology, and comparisons of the COBE satellite's observations of fluctuations in the Cosmic Microwave Background Radiation (CMBR) temperature to predicted fluctuations for closed hyperbolic manifolds have been made [4]. Much effort has gone into uncovering good signatures for such topology [5, 6]. The effort is complicated by the fact that there are infinitely many different possible topologies for negatively curved manifolds. Moreover, a large, perhaps infinite number of these have small enough closed loops (in at least some directions) that they could in principle yield observable consequences. Therefore the best signatures must allow general searches for topology and not just allow us to tell whether the universe is a particular manifold.

One such generic topology search algorithm utilizes the very robust observation that the existence of topology will result in the existence of pairs of circles on the sky which have highly correlated patterns of CMBR temperature fluctuations [13].

Another suggestion, made by Levin et al [1], is that flat spots (regions with suppressed long-wavelength fluctuations in temperature) will appear in the CMBR sky, in particular in compact hyperbolic manifolds. Levin et al examined one particular hyperbolic manifold, the so-called horn topology (which is not compact), and discovered that down the direction of the horn such flat spots do indeed appear. To understand the suggestion that these flat spots are generic one must realize that hyperbolic manifolds of non-trivial topology correspond to tilings of the covering space of hyperbolic geometry, the usual "open" \mathbf{H}^3 . A compact hyperbolic manifold is then a tiling whose fundamental or Dirichlet domain does not extend to spatial infinity. Such compact hyperbolic manifolds are however constructed by a process of Dehn surgery on so-called cusped manifolds, which extend to infinity at a finite number of isolated points, called cusps. The cusp portions of the cusped manifolds are very much like the horn topology in that in both cases the cross-section of the manifold narrows exponentially as one moves down the horn/cusp toward spatial infinity. As the manifold narrows, geodesics can readily wrap around the horn/cusp a large number of times and so smooth out any features. The suggestion that the flat spots seen in the horn topology may be more generic, assumes that the Dehn surgery required to turn the cusped manifold into the compact manifold is sufficiently gentle so as to preserve this evidence of the cusps of the parent cusped manifold.

In this paper we will try to see just how far the analogy between cusped and horned manifold can take us – how flat are the flat spots which would appear in the cusped manifold. This represents the flattest that one could expect the flat spots in the daughter cusp-free manifold to be. We will show that although the cusps *do* produce flat spots they are generically not quite so prominent as those produced in the horn topology.

2 Modes on the Horosphere

In a small volume cusped hyperbolic manifold, it is difficult to calculate the eigenmodes of the wave operator which contribute to variations in the CMBR (although see [7, 8, 9, 10]). However, since all that interests us is whether or not there is a flat spot on the CMBR in the vicinity of a

cusped, we need not solve the full problem. Instead, we find how the topology affects the modes on the surface of last scattering (SLS) near the cusp.

To compute these modes, we need to choose a model of \mathbf{H}^3 in which to compute. There are many models of \mathbf{H}^3 . The most common representation of \mathbf{H}^3 is Poincare's model, which is the unit ball in \mathbf{R}^3 with the metric $ds^2 = \frac{4}{(1-r^2)^2} dx^2$. Here dx^2 is the normal metric of \mathbf{R}^3 and r is the distance from the origin. In this model, geodesics are diameters of the unit sphere and circular arcs perpendicular to the surface of the unit sphere [11]. Of more use to us will be the hyperboloid model of \mathbf{H}^3 , which is the set of points in \mathbf{R}^{1+3} on the upper sheet of the hyperboloid $-1 = -x_0^2 + x_1^2 + x_2^2 + x_3^2$. The distance d between two points x, y in this model is $d = \text{arccosh}(-x \circ y)$, where $x \circ y = -x_0 y_0 + x_1 y_1 + x_2 y_2 + x_3 y_3$ is the Lorentz dot product of two points in \mathbf{R}^{1+3} . Geodesics in the hyperboloid model have the form $\lambda(t) = x \cosh(t) + y \sinh(t)$, where x is a point on the hyperboloid and y is a unit vector in \mathbf{R}^{1+3} orthogonal to it [12]. Finally, we will also make use of the Klein model of \mathbf{H}^3 . This is obtained from the hyperboloid model by projecting the point (x_0, x_1, x_2, x_3) to the point $(\frac{x_1}{x_0}, \frac{x_2}{x_0}, \frac{x_3}{x_0})$. Geodesics in the Klein model are open chords of the unit ball [11].

We now use a horosphere to find the modes near the cusp. A horosphere is a sphere inside and tangent to the unit sphere in the Poincare model of H^3 . We consider the horosphere tangent at the cusp that goes through the point on the SLS in the direction of the cusp. On the horosphere, the transformation group of the manifold restricts to a Euclidean similarity group [12]. We calculate the modes of this group, and use them as an approximation to the modes on the SLS. By comparing the density of these modes to those of a corresponding patch of open sky, we get an estimate of any suppression caused by the topology.

We did this calculation on a particular cusped manifold – number m003 from the Snappea census of cusped manifolds [3]. This manifold is obtained by gluing the faces of two ideal tetrahedra¹ together and has a volume $V \approx 2.0299$, in units of the curvature radius cubed. The Dirichlet domain we considered (cf. figure 1) is centered on one of the tetrahedra, with the other tetrahedron split into quarters which are attached to the faces of the first tetrahedron. The resulting figure has four ideal vertices, four finite vertices, eighteen edges, and twelve faces. Numbering the ideal vertices 1, 2, 3, and 4, we can associate each finite vertex with the ideal vertices which it shares edges with. The finite vertices are numbered 5, 6, 7, and 8, with vertex 5 forming edges with vertices 1, 2, and 3, vertex 6 forming edges with vertices 1, 2, and 4, vertex 7 forming edges with vertices 2, 3, and 4, and vertex 8 forming edges with vertices 1, 3, and 4. Each face can be identified by its three vertices. In m003, the faces are glued in the pattern 125-347, 237-348, 138-246, 148-135, 146-247, and 126-235. There are then six classes of faces, six classes of edges and two classes of vertices.

In the Klein model, the vertices of m003 are

$$\begin{aligned} v_1 &= \left(-\frac{1}{\sqrt{3}}, -\frac{1}{\sqrt{3}}, \frac{1}{\sqrt{3}}\right), & v_2 &= \left(\frac{1}{\sqrt{3}}, -\frac{1}{\sqrt{3}}, -\frac{1}{\sqrt{3}}\right), \\ v_3 &= \left(\frac{1}{\sqrt{3}}, \frac{1}{\sqrt{3}}, \frac{1}{\sqrt{3}}\right), & v_4 &= \left(-\frac{1}{\sqrt{3}}, \frac{1}{\sqrt{3}}, -\frac{1}{\sqrt{3}}\right), \\ v_5 &= \left(\frac{\sqrt{3}}{5}, -\frac{\sqrt{3}}{5}, \frac{\sqrt{3}}{5}\right), & v_6 &= \left(-\frac{\sqrt{3}}{5}, -\frac{\sqrt{3}}{5}, -\frac{\sqrt{3}}{5}\right), \\ v_7 &= \left(\frac{\sqrt{3}}{5}, \frac{\sqrt{3}}{5}, -\frac{\sqrt{3}}{5}\right), & \text{and } v_8 &= \left(-\frac{\sqrt{3}}{5}, \frac{\sqrt{3}}{5}, \frac{\sqrt{3}}{5}\right). \end{aligned} \quad (2)$$

The six generators of the transformation group are, in the hyperboloid model,

$$a_0 = \begin{pmatrix} \frac{7}{4} & -\frac{\sqrt{3}}{4} & -\frac{3\sqrt{3}}{4} & \frac{\sqrt{3}}{4} \\ \frac{\sqrt{3}}{4} & -\frac{1}{4} & -\frac{3}{4} & -\frac{3}{4} \\ -\frac{3\sqrt{3}}{4} & \frac{3}{4} & \frac{5}{4} & -\frac{3}{4} \\ \frac{\sqrt{3}}{4} & \frac{3}{4} & -\frac{3}{4} & \frac{1}{4} \end{pmatrix}, \quad a_1 = \begin{pmatrix} \frac{7}{4} & \frac{\sqrt{3}}{4} & -\frac{3\sqrt{3}}{4} & -\frac{\sqrt{3}}{4} \\ \frac{3\sqrt{3}}{4} & \frac{3}{4} & -\frac{5}{4} & -\frac{3}{4} \\ \frac{\sqrt{3}}{4} & -\frac{3}{4} & -\frac{3}{4} & -\frac{1}{4} \\ -\frac{\sqrt{3}}{4} & -\frac{1}{4} & \frac{3}{4} & -\frac{3}{4} \end{pmatrix},$$

¹An *ideal* polyhedron is one with only ideal vertices. An ideal vertex in the Poincare or Klein model is a vertex located on the unit sphere. A *finite* vertex is a vertex which is not ideal.

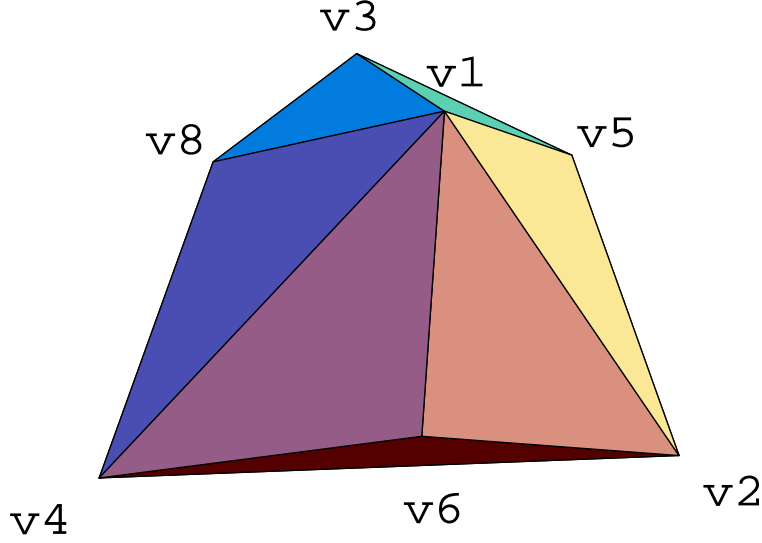


Figure 1: The Dirichlet domain of the manifold m003 in the Snappea census centered at the origin of the Klein model.

$$\begin{aligned}
 a_2 &= \begin{pmatrix} \frac{7}{4} & \frac{\sqrt{3}}{4} & \frac{\sqrt{3}}{4} & \frac{3\sqrt{3}}{4} \\ -\frac{\sqrt{3}}{4} & -\frac{1}{4} & \frac{3}{4} & -\frac{3}{4} \\ \frac{\sqrt{3}}{4} & -\frac{3}{4} & \frac{1}{4} & \frac{3}{4} \\ \frac{3\sqrt{3}}{4} & \frac{3}{4} & \frac{3}{4} & \frac{5}{4} \end{pmatrix}, & a_3 &= \begin{pmatrix} \frac{7}{4} & -\frac{\sqrt{3}}{4} & \frac{\sqrt{3}}{4} & -\frac{3\sqrt{3}}{4} \\ -\frac{3\sqrt{3}}{4} & \frac{3}{4} & -\frac{3}{4} & \frac{5}{4} \\ \frac{\sqrt{3}}{4} & -\frac{1}{4} & -\frac{3}{4} & -\frac{3}{4} \\ \frac{\sqrt{3}}{4} & \frac{3}{4} & \frac{1}{4} & -\frac{3}{4} \end{pmatrix}, \\
 a_4 &= \begin{pmatrix} \frac{7}{4} & -\frac{\sqrt{3}}{4} & -\frac{\sqrt{3}}{4} & \frac{3\sqrt{3}}{4} \\ -\frac{3\sqrt{3}}{4} & \frac{3}{4} & \frac{3}{4} & -\frac{5}{4} \\ -\frac{\sqrt{3}}{4} & \frac{1}{4} & -\frac{3}{4} & -\frac{3}{4} \\ -\frac{\sqrt{3}}{4} & -\frac{3}{4} & \frac{1}{4} & -\frac{3}{4} \end{pmatrix} & \text{and} & a_5 &= \begin{pmatrix} \frac{7}{4} & -\frac{3\sqrt{3}}{4} & \frac{\sqrt{3}}{4} & -\frac{\sqrt{3}}{4} \\ -\frac{\sqrt{3}}{4} & \frac{3}{4} & \frac{3}{4} & \frac{1}{4} \\ -\frac{3\sqrt{3}}{4} & \frac{5}{4} & -\frac{3}{4} & \frac{3}{4} \\ -\frac{\sqrt{3}}{4} & \frac{3}{4} & -\frac{1}{4} & -\frac{3}{4} \end{pmatrix}.
 \end{aligned} \tag{3}$$

These generators are orientation preserving and satisfy the six relations

$$\begin{aligned}
 a_0 a_1^{-1} a_5^{-1} &= 1, & a_3 a_2 a_4^{-1} &= 1, \\
 a_1 a_2 a_4 &= 1, & a_0 a_1 a_3 &= 1, \\
 a_5 a_0 a_4^{-1} &= 1, & \text{and} & a_2 a_5 a_3^{-1} = 1.
 \end{aligned} \tag{4}$$

The Euclidean similarity group of a horosphere centered on a cusp is a tiling of the Euclidean plane with hexagons. There are four elements in the tiling, one from each ideal vertex of the domain. The tiling is shown in figure 1. To calculate the eigenmodes of the wave operator on the tiling, the rectangular domain and the axes shown in figure 1 were used. The similarity group of this tiling is generated by the two transformations $T_1(x, y) = (x + L, y)$, $T_2(x, y) = (x + \frac{L}{2}, y + \frac{\sqrt{3}L}{2})$, and the modes $\phi(x, y)$ of the tiling are solutions of the Helmholtz (wave) equation under the two boundary conditions $\phi(T_i(x, y)) = \phi(x, y)$ for $i = 1, 2$. A straightforward argument shows that the normal modes that satisfy these boundary conditions have wavevectors \vec{k} of the form

$$\vec{k} = \frac{2\pi}{L} \left[n \left(1, -\frac{1}{\sqrt{3}} \right) + m \left(0, \frac{2}{\sqrt{3}} \right) \right] \tag{5}$$

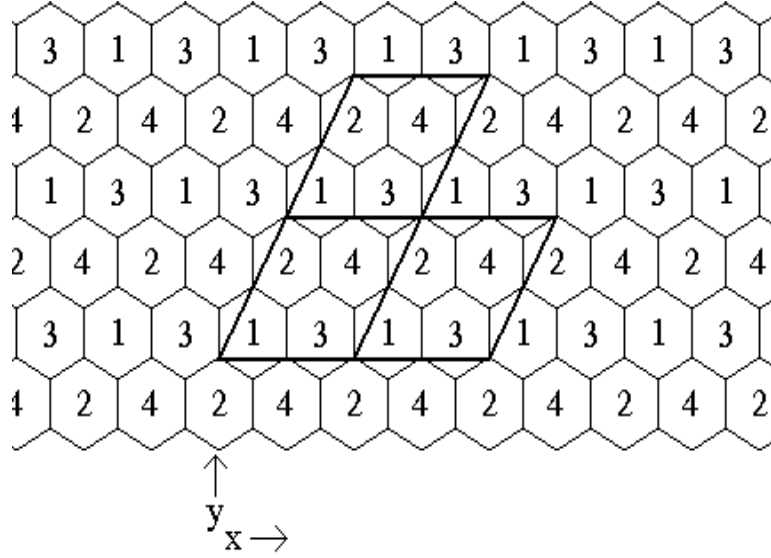


Figure 2: Hexagonal tiling of the horosphere with the rectangular domain used to calculate the modes of the wave equation superimposed.

with n, m arbitrary integers. The shortest nonzero \vec{k} modes have $k_{min} = \frac{2\pi}{L} \frac{2}{\sqrt{3}}$. This corresponds to a maximum wavelength $\lambda_{max} = \frac{2\pi}{k_{min}} = \frac{\sqrt{3}L}{2}$ for solutions with these boundary conditions.

3 From Horosphere to Sphere of Last Scatter

We have now found the wavelengths of the modes on the portion of the SLS that is tiled like the horosphere. To find L and calculate how much of the SLS is tiled, we computed the intersections of the SLS with the edges of the domains in the tiling. The size and maximum wavelength of flat spots on the CMB varies from point to point in the manifold, depending on how far down the cusp a point is. To account for this, we chose to consider the SLS of three points: the point $(1, 0, 0, 0)$ in the hyperboloid model, the point at the radius of half volume (0.61 in units of the curvature radius R_{curv}) towards the cusp from $(1, 0, 0, 0)$, and the point at a distance equal to the curvature radius towards the cusp from $(1, 0, 0, 0)$. The point $(1, 0, 0, 0)$ is at the center of the Dirichlet domain we considered, at a distance $0.58R_{curv}$ from the nearest face. It is positioned as far from the small regions down the cusp as possible, so it has the smallest amount of its SLS tiled and the largest cusp wavelength cutoff of the points in the manifold. The radius of half volume is calculated by determining the radius of a sphere centered on $(1, 0, 0, 0)$ whose intersection with the Dirichlet domain has a volume half that of the manifold. The point at the radius of half volume is closer to the small cusp regions than approximately half of the points in the manifold, so it has a spot size and wavelength cutoff which we take to be representative of an average point of the manifold. It is a distance $0.33R_{curv}$ from the nearest face. The point at the curvature radius distance is well down the cusp, with a distance of only $0.22R_{curv}$ from the nearest face, so we will use it to estimate the spot size and shortest wavelength cutoff of points in the manifold which are further down the cusp than average. The radius of the last scattering

surface in units of the curvature scale[13] is a function of Ω_0 :

$$R_{SLS} \approx R_{curv} \text{arccosh} \left(\frac{2 - \Omega_0}{\Omega_0} \right). \quad (6)$$

Using $\Omega_0 = 0.3$ and $R_{curv} \equiv 1$, we get $R_{SLS} \approx 2.4$. (This is actually the radius of the particle horizon, which is marginally larger than the radius of the SLS.)

In the domain centered on $(1, 0, 0, 0)$ in the hyperboloid model, a point p on the edge between the ideal vertices v_i and v_j satisfies the equation $p(r) = e_{ij} \cosh r + t_{ij} \sinh r$, where e_{ij} is the center of the edge ij and t_{ij} is the unit vector tangent to the hyperboloid pointing along the edge. The e_{ij} and t_{ij} are:

$$\begin{aligned} e_{12} &= \left(\sqrt{\frac{3}{2}}, 0, -\sqrt{\frac{1}{2}}, 0 \right), & t_{12} &= \left(0, -\sqrt{\frac{1}{2}}, 0, \sqrt{\frac{1}{2}} \right) \\ e_{13} &= \left(\sqrt{\frac{3}{2}}, 0, 0, \frac{1}{\sqrt{2}} \right), & t_{13} &= \left(0, -\frac{1}{\sqrt{2}}, -\frac{1}{\sqrt{2}}, 0 \right) \\ e_{14} &= \left(\sqrt{\frac{3}{2}}, -\frac{1}{\sqrt{2}}, 0, 0 \right), & t_{14} &= \left(0, 0, -\frac{1}{\sqrt{2}}, \frac{1}{\sqrt{2}} \right) \\ e_{23} &= \left(\sqrt{\frac{3}{2}}, \frac{1}{\sqrt{2}}, 0, 0 \right), & t_{23} &= \left(0, 0, -\frac{1}{\sqrt{2}}, -\frac{1}{\sqrt{2}} \right) \\ e_{24} &= \left(\sqrt{\frac{3}{2}}, 0, 0, -\frac{1}{\sqrt{2}} \right), & t_{24} &= \left(0, \frac{1}{\sqrt{2}}, -\frac{1}{\sqrt{2}}, 0 \right) \\ e_{34} &= \left(\sqrt{\frac{3}{2}}, 0, \frac{1}{\sqrt{2}}, 0 \right), & t_{34} &= \left(0, \frac{1}{\sqrt{2}}, 0, \frac{1}{\sqrt{2}} \right) \end{aligned} \quad (7)$$

The edges between a finite vertex v_i and an ideal vertex v_j satisfy the equation $p(r) = v_i \cosh r + t_{ij} \sinh r$, where v_i is the finite vertex and t_{ij} is the unit vector tangent to the hyperboloid in the direction of the ideal vertex v_j . The v_i are stated above in equation 2. The t_{ij} are:

$$\begin{aligned} t_{51} &= \left(-\frac{1}{4}, -\frac{7}{4\sqrt{3}}, -\frac{1}{4\sqrt{3}}, \frac{1}{4\sqrt{3}} \right), & t_{52} &= \left(-\frac{1}{4}, \frac{1}{4\sqrt{3}}, -\frac{1}{4\sqrt{3}}, -\frac{7}{4\sqrt{3}} \right) \\ t_{53} &= \left(-\frac{1}{4}, \frac{1}{4\sqrt{3}}, \frac{7}{4\sqrt{3}}, \frac{1}{4\sqrt{3}} \right), & t_{61} &= \left(-\frac{1}{4}, -\frac{1}{4\sqrt{3}}, -\frac{1}{4\sqrt{3}}, \frac{7}{4\sqrt{3}} \right) \\ t_{62} &= \left(-\frac{1}{4}, \frac{7}{4\sqrt{3}}, -\frac{1}{4\sqrt{3}}, -\frac{1}{4\sqrt{3}} \right), & t_{64} &= \left(-\frac{1}{4}, -\frac{1}{4\sqrt{3}}, \frac{7}{4\sqrt{3}}, -\frac{1}{4\sqrt{3}} \right) \\ t_{72} &= \left(-\frac{1}{4}, \frac{1}{4\sqrt{3}}, -\frac{7}{4\sqrt{3}}, -\frac{1}{4\sqrt{3}} \right), & t_{73} &= \left(-\frac{1}{4}, \frac{1}{4\sqrt{3}}, \frac{1}{4\sqrt{3}}, \frac{7}{4\sqrt{3}} \right) \\ t_{74} &= \left(-\frac{1}{4}, -\frac{7}{4\sqrt{3}}, \frac{1}{4\sqrt{3}}, -\frac{1}{4\sqrt{3}} \right), & t_{81} &= \left(-\frac{1}{4}, -\frac{1}{4\sqrt{3}}, -\frac{7}{4\sqrt{3}}, \frac{1}{4\sqrt{3}} \right) \\ t_{83} &= \left(-\frac{1}{4}, \frac{7}{4\sqrt{3}}, \frac{1}{4\sqrt{3}}, \frac{1}{4\sqrt{3}} \right), & t_{84} &= \left(-\frac{1}{4}, -\frac{1}{4\sqrt{3}}, \frac{1}{4\sqrt{3}}, -\frac{7}{4\sqrt{3}} \right) \end{aligned} \quad (8)$$

Every domain in the tiling can be obtained by applying an element of the transformation group of the tiling to the domain centered at $(1, 0, 0, 0)$. Applying the transformation of a domain to these edge parametrizations yields a parametrization of the edges of that domain.

The intersection of any edge with the SLS of any point P_c can now be found by numerically solving the equation $D(p(r), P_c) = 2.4$, where $D(x, y)$ is the distance between two points in the hyperboloid model and $p(r)$ is the parametrization of the edge. All intersections of edges with the SLS of each of the three points in the vicinity of cusp 1 of the domain centered at $(1, 0, 0, 0)$ were calculated. The results for the point $(1, 0, 0, 0)$ are shown in figure 2, which plots the pattern of domain edge intersections as seen on the night sky. The connected points are intersections of the edges of the Dirichlet domain with the SLS. The large dot in the center is the geodesic traveling straight down the cusp. The line segments from the cusp show the scale of the diagram, and are of length 4.8 and 8.8 degrees. The diagram shows that the tiling of the sky within a half-angle of 4.8 degrees has little distortion and will have modes similar to the horosphere. The outer hexagons shown are falling back into the large part of the manifold, and can no longer be approximated by tiled horosphere hexagons. The side length of the central hexagon is 0.65 degrees. The half volume point and the curvature radius point have disks with radii of 5.4 and 6.2 degrees and central hexagons with side lengths of 0.35 and 0.24 degrees.

We used these hexagon side lengths l_h for the scale $L = 2\sqrt{3}l_h$ of the tiling of the horosphere to find $k_{min} = \frac{2\pi}{L} \frac{2}{\sqrt{3}}$ and $\lambda_{max} = \frac{2\pi}{k_{min}}$ for the modes on the horosphere. The point $(1, 0, 0, 0)$

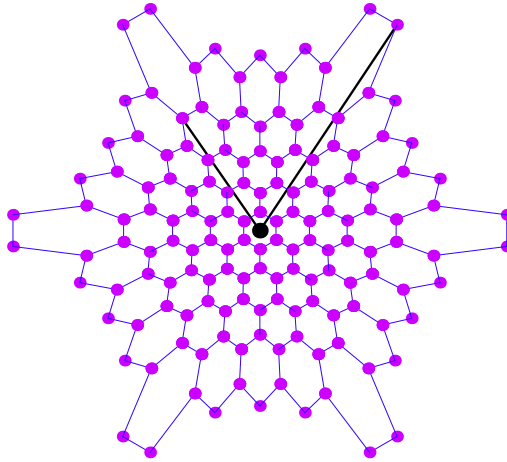


Figure 3: Tiling of space as projected onto the night sky.

has a $\lambda_{max} = 2.0$ degrees, so the longest wavelength mode on the SLS for the point $(1, 0, 0, 0)$ in the vicinity of the cusp is approximately 2.0 degrees.

In the absence of non-trivial topology, this region will have the modes of a disc of radius 4.8 degrees, which have wavelengths $\lambda_n = \frac{2\pi \cdot 4.8}{J_{m,n}}$ degrees, where $J_{m,n}$ is the n th zero of the m th cylindrical Bessel function. The longest wavelength mode will have $\lambda_{max} = 12.5$ degrees.

Comparing the longest wavelength of the drum, 12.5 degrees, and the longest wavelength of the horosphere, 2.0 degrees, shows that the topology reduces the longest wavelength to about 0.16 of its expected value. So the SLS of the point $(1, 0, 0, 0)$ exhibits a flat spot of approximately 4.8 degrees.

The half volume point has a longest horosphere wavelength of 1.05 degrees and a longest disc wavelength of 14.1 degrees. Here the longest wavelength is reduced to about 0.07 of its expected value on a spot of half angle 5.4 degrees.

The curvature radius point has horosphere modes of longest wavelength 0.72 degrees and disc modes of longest wavelength 16.1 degrees. The longest wavelengths is reduced to 0.04 of its normal value on a spot of half angle 6.2 degrees.

These results depend on having a relatively small value of Ω_0 . As an example of this, the corresponding calculations using this method with an $\Omega_0 = 0.9$, which has an $R_{sls} \approx 0.65 R_{curv}$ yield a null result for flattening. The point $(1, 0, 0, 0)$ has only one hexagon in its tiling, with a sidelength of 40 degrees. The half volume radius point has seven hexagons in its tiling, with a central side length of 19 degrees and serious distortions of the outer hexagons. The curvature radius point also has a distorted tiling of seven hexagons, with a central side length of 11.4 degrees. None of these points exhibits an extensive regular tiling of the SLS in the direction of the cusp, so our calculations do not predict a flat spot due to the cusp for $\Omega_0 = 0.9$.

Finally, Gaussian random fields do have flat spots, arising purely from statistical fluctuations. However, in order for a statistical flat spot to be confused with one of topological origin, many modes would have to have an amplitude much smaller than the mean. For example, in order to create a spot in which the wavelength of the longest observed mode is only 7% of the expected value approximately 600 modes would have to have statistically small amplitudes. (Since $\pi \times (\frac{100}{7})^2 \simeq 600$.)

4 Conclusion

In reference [1], the horn topology was shown to have flat spots which could, in principle cover a large portion of the CMBR. By estimating the modes on the surface of last scatter for a point at half volume down the cusp, we have found that the cusped manifold m003 from the Snappea census has a flat spot of about five degrees with longest wavelengths cut to about 0.07 of normal

when $\Omega_0 = 0.3$ for an average observer. Calculations with two other points show that the flat spot is larger and the wavelength cutoff is more pronounced at points farther down the cusp and smaller and less pronounced for points nearer the center of the manifold. The calculations suggest that similar spots will be seen in any cusped manifold at points which are close enough to a cusp. A cusped manifold will only be able to avoid having spots by being large enough that most points are far from cusps, so any small volume cusped hyperbolic manifold should have observable flat spots. Such flat spots are unlikely to be mere statistical fluctuations of the temperature field. This supports visible flat spots in the CMBR fluctuation maps as a likely, though not necessarily automatic, feature in a hyperbolic universe with non-trivial topology.

References

- [1] Levin J J Barrow J D Bunn E F and Silk J 1997 *Phys. Rev. Lett.* **79** 974
- [2] Cornish N Spergel D N and Starkman G D 1998 *Phys. Rev.* **D57** 5982
- [3] Weeks J *SnapPea*: A computer program for creating and studying hyperbolic 3-manifolds, available at <http://www.geom.umn.edu:80/software>
- [4] Bond JR Pogosyan D and Souradeep T 1998 *Class. Quantum Grav.* **15** 2573
- [5] Starkman G D 1998 *Class. Quantum Grav.* **15** 2529
- [6] Luminet J-P and Roukema B F 1999 in *Theoretical and Observational Cosmology* NATO Advanced Study Institute, Cargèse 1998, ed. Lachiéze-Rey M *et al.*
- [7] Inoue K T 1998 *Preprint* astro-ph/9810034
- [8] Aurich R 1999 *Preprint* astro-ph/9903032
- [9] Cornish N and Spergel D N *Preprint* math.DG/9906017
- [10] Steil G 1999 in *Emerging Applications of Number Theory* ed Hejhal, Friedman, Gutzwiller and Odlyzko (New York: Springer)
- [11] Thurston W 1997 *Three Dimensional Geometry and Topology, Vol. 1* (Princeton, NJ: Princeton University Press)
- [12] Ratcliffe J G 1994 *Foundations of Hyperbolic Manifolds* (New York: Springer Verlag)
- [13] Cornish N Spergel D N and Starkman G D 1998 *Class. Quantum Grav.* **15** 2657